https://doi.org/10.2352/ISSN.2169-4451.2017.32.452

Altering the Bubble Release of Reactive Inkjet Printed Silk Micro-rockets

David A. Gregory[1], Yu Zhang[1], Patrick J. Smith[2], Stephen J. Ebbens[1], Xiubo Zhao[1]*

1. Department of Chemical and Biological Engineering, University of Sheffield, Sheffield, UK
2. Department of Mechanical Engineering, University of Sheffield, Sheffield, UK
**Author for correspondence: xiubo.zhao@sheffield.ac.uk*

Abstract

A novel approach of using layer-by-layer (LBL) reactive inkjet printing (RIJ) of regenerated silk fibroin (RSF) was used to generate micron-sized silk rockets which have the enzyme catalase immobilised inside the silk scaffold structure and use the catalase enzyme to drive their motion in samples containing H_2O_2 as a fuel. By using the LBL printing approach we show that is it possible to generate 3D structures where different materials can be incorporated into the structure at defined locations. The use of silk together with an inkjet printing method has great potential to easily incorporate different enzymes, proteins, chemicals or other biomolecules and build versatile devices by entrapping them into the silk scaffold. This allows us to generate small-scale devices that can generate thrust via catalytic reactions within fluidic environments for potential applications including environmental monitoring and remediation, in vivo drug delivery and repair, and lab-on-a-chip diagnostics. In contrast, current manufacturing processes of micromotors often use slow and lengthy production processes (e.g. evaporation) combined with expensive materials such as platinum. The location of catalyst on these devices has been shown to influence trajectory behaviour, which is not easy to control using conventional methods. Furthermore devices using platinum as a catalyst can undergo biofouling thus inhibiting their catalytic reactions. By using biocompatible silk scaffolds, created by RIJ, the devices generated here have the potential to overcome all these problems.

Introduction

Over the last ten years the production of small-scale devices that are able to generate autonomous motion via catalytic reactions within fluidic environments has become an increasingly active field of research. [1-5] The potential applications for these devices, including Lab-on-a-Chip diagnostics, [6] environmental monitoring, water remediation, [7-11] as well as *in vivo* drug delivery and repair [12], have been one of the key aspects why these devices have received increasing attention. It is however important to note that current production methods and materials have many limitations. A large proportion of devices are based on lithographic approaches in order to control the shape and catalytic distributions, which means that there are many limits to the design of devices particularly in respect to future scalability. Further to this, these devices frequently use expensive metals such as gold and platinum which require high vacuum evaporation systems or complex chemical processes in order to produce thin metal coatings. In addition, these metal coatings are highly susceptible to biofouling, thus inhibiting their catalytic reactions and therefore meaning that the particles cannot swim in biological fluids without the addition of surfactants, which are undesirable.

In the pursuit of effective propulsive devices via chemical reactions it is of vital importance to be able to control the distribution of catalyst as well as the shape of the devices. [13] There are two main propulsion mechanisms for catalytic micro-motors: Firstly, they can be moved by phoretic phenomena, for these an asymmetric distribution of catalyst is essential. [3, 4, 14-17] The second mechanism is by momentum transfer during gas bubble detachment (bubble propulsion). [18-20] Here catalyst location has been shown to improve directionality. [13] The devices we investigate here move through the latter mechanism. In order to make devices that contain the required distribution of catalysts, often difficult and time-consuming methods such as the evaporation of metals (e.g. platinum) are necessary. [5, 21] Platinum is often a choice of catalyst as it catalyses the decomposition of hydrogen peroxide (H_2O_2) into water and oxygen. In contrast to platinum based micro-motors there have been examples of micro-motors that use the enzyme catalase as a catalyst, however current micro-motors using enzymes as catalysts predominantly also need to use of metal surfaces for the initial covalent attachment via complex chemical reactions, and are once again time consuming as well as not achieving very high catalytic reactivity. [22-24]

Pursuing devices that have the ability to provide functions for cargo transport [8] equally needs well-defined structures. Because of significant challenges in current technologies to produce these devices, it at present has not been possible to rapidly design and test various designs easily and thus slowing down the development of these devices for future applications. Recent developments in the swimming field to produce new production methods has seen the device manufacture via screen printing of platinum powered devices [25, 26], but here physical masks or advanced digital micro-mirror devices [26] have to be used. Further issues with catalytic micro-motors containing platinum as a catalyst are that these devices are highly susceptible to contamination by hydrocarbons [27] and thiols [28] as well as surface fouling in biological fluids such as human serum where proteins are absorbed to the metal surface in habiting the catalytic reactions. In order for these devices to function in bio fluids undesirable additives such as surfactants have to be added [29] to reduce the fouling behavior. [30]

In contrast to this, here we show the possibility of producing rapidly moving autonomous bubble-propulsive silk micro-rockets via RIJ [31] of RSF, an FDA approved material, which are powered by the catalytic enzyme catalase. These devices show high biocompatibility and usability for a wide range of applications.

As shown representatively in the schematic in **Figure 1** the catalase enzyme contained within the silk lattice structure decomposes the hydrogen peroxide fuel into water and oxygen

(Eq. {1}), which are released from the silk rockets as bubbles allowing for the bubble propulsion mechanism to take place.

Silk fibroin is a versatile material, which has been known for its strong mechanical properties, [32] easy processing [33] as well as its, excellent biocompatibility [34] and tunable biodegradability. [35] RIJ allows the printing of methanol on top of the printed silk ink transforming it from water soluble ***Silk I*** (random coil structure) state to water insoluble ***Silk II*** (β-sheet secondary structure) state. [36-38] Therefore, if an enzyme such as catalase is mixed with the water soluble silk ink (***Silk I***) and this mixture is then exposed to methanol the enzyme molecules are entrapped into the newly formed silk scaffold (***Silk II***) and thus securely encapsulated within the solid silk structure. [39]

$$2H_2O_{2(l)} \xrightarrow{Catalase} 2H_2O_{(l)} + O_{2(g)} \qquad \{1\}$$

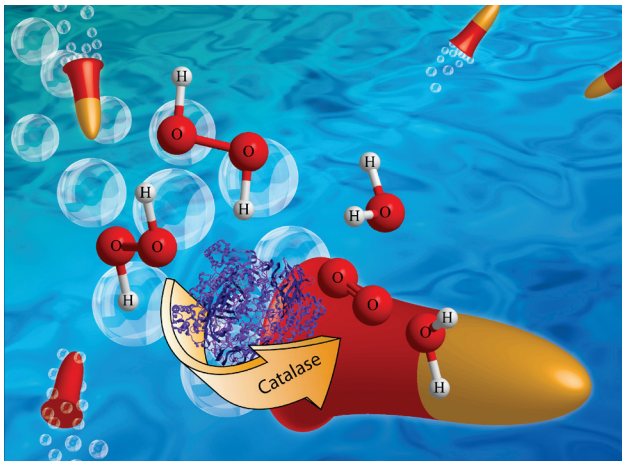

Figure 1. *Schematic representation of inkjet-printed silk micro-rockets containing the enzyme catalase which decomposes hydrogen peroxide fuel molecules into water and molecular oxygen (see Eq. {1}). The produced oxygen bubbles therefore induce the silk micro-rocket's propulsive motion. Red half of the Janus micro-rocket is the silk /PEG_{400}/ catalase/ containing segment whereas the orange half is the segment only containing silk/PEG_{400}.*

Results and Discussion

In order to achieve a rocket-like (column) structure it was necessary to deploy a layer-by-player RIJ printing approach. **Figure 2** shows a schematic representation of the final design used for Janus micro-rockets which we recently reported (in Small [39]). Here we look into the aspects involving how silk concentrations and the addition of PEG_{400} along with PMMA barrier layer affect the bubble release and swimming behaviour of our rockets. The process of printing RSF silk solutions via RIJ is described in more detail in Y. Zhang's paper that will be presented at this conference as well.

In order to fabricate 3D silk scaffolds, which were capable of generating stable long lasting swimming devices silk concentrations were important to consider. Observations showed that at concentrations below 20 mg/ml of RSF swimmers when placed into liquid showed sponge-like features, which were not rigid and deformed more during catalysis. After testing a variety of concentrations it appeared that at 30 mg/ml a good rigid silk structure was present that would remain structurally sound, long past the experimental tests. In a next step it was important to ensure bubble detachment was efficient which was tuned by adding PEG_{400}.

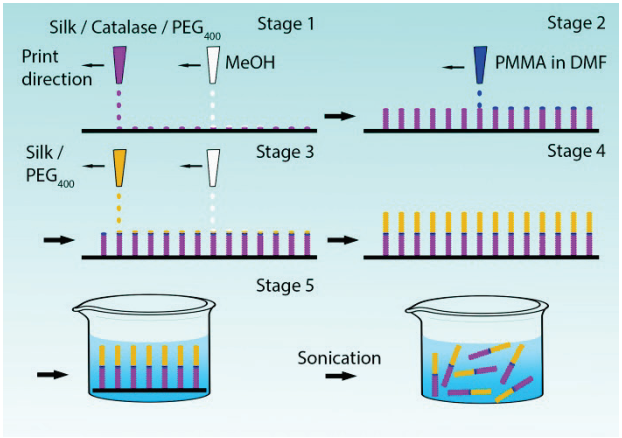

Figure 2*. Schematic of the RIJ process for manufacturing catalytic micro-rockets, optimized [39]. Stage 1: Alternate printing of a silk/catalase/PEG (purple) ink and a methanol (white) ink (transforms printed silk ink from Silk I to Silk II) to build the catalytically active base of the micro-rocket. Stage 2: 10 layers of PMMA (blue) ink are deposited to act as a divider between the two halves of the rocket (to stop the penetration of oxygen bubbles generated into the inactive part of the micro-rocket). Stage 3: The second half of the rocket is deposited as in stage 1, but a silk/PEG (orange) ink is now used. Stage 4: Manufacture complete, substrate is immersed into the fluidic swimming media. Stage 5: Ultrasonication is used to detach the micro-rockets from the substrate.*

Effects of PEG_{400} on the silk micro-rockets

PEG_{400} plays an important role in achieving successful bubble detachment from the silk micro-rockets. **Figure 3A** clearly shows that silk rockets not containing PEG_{400} ended up generating one large bubble which would eventually burst, but only after growing to a very large size which in turn did not generate the continuous desired propulsion. By adding PEG_{400} into the RSF ink frequent bubble release was achieved allowing the swimmers to undergo bubble propulsion, as can be seen from **Figure 3B**. The addition of PEG_{400} to the silk rockets altered the bubble release efficiency, this means it is possible to fabricate rockets with a lower amount of PEG_{400} to alter the bubble release efficiency. It appears that PEG_{400} alters the hydrophobicity of the silk rockets [40] (see **Figure 4**) and therefore bubbles detach more readily, where the addition of more PEG_{400} decreases the hydrophobicity. [41] Further to this, an observation was made that for silk inks not containing any PEG_{400} enzyme accumulation around the orifice of the print nozzle was much stronger than for inks containing PEG_{400}, meaning that more frequent cleaning of the nozzle was necessary.

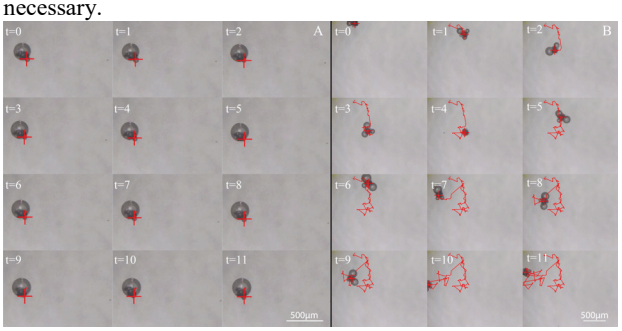

Figure 3*. (A) Silk swimmer containing catalase enzymes but with no PEG_{400} blended in showing the bubble detachment / popping issue (Image is taken from above so looking down onto the particles). (B) Silk swimmer containing PEG_{400} showing efficient bubble release.*

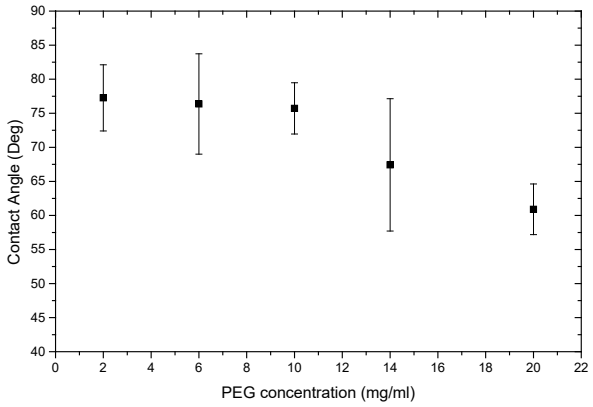

Figure 4. *Contact angle measurements of 5 layers of spun cast silk (20 mg/ml) with different concentrations of PEG_{400} blended in.*

As the printed silk scaffolds are of porous nature, this allows for enzyme molecules locked within the centre of the rocket to still be able to decompose hydrogen peroxide, increasing the overall accessibility of the enzyme. This means the amount of enzyme that is able to catalyse the reaction is far greater than that of enzyme monolayer coverage of other previously described devices. However this also generates a problem in regards to fabricating micro-rockets which have an active and an inactive area. As shown in **Figure 5A** silk rockets made up of an active and a non-active segment (with and without catalytic enzyme) show to produce bubbles across the entire particle, we assume due to the porosity of the silk lattice structure oxygen leeches through the entire structure and escapes across all sides, where the active side still shows a bias for more bubbles being released, this scenario is far from ideal. In contrast if a PMMA barrier layer of a mere 10 printed layers is introduced between the two segments of the Janus particles the leeching of bubbles between the two segments stops and a highly directional trajectory is generated due to bubbles being release from only the active side of the Janus silk micro-rockets (**Figure 5 B**).

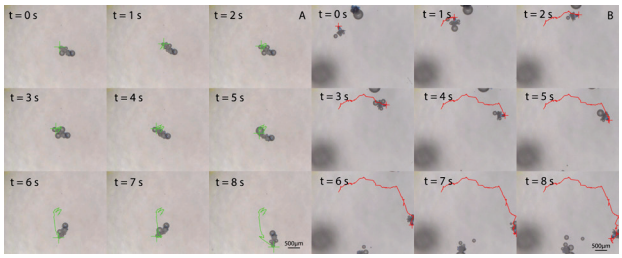

Figure 5. *(A) Janus Silk swimmers made up of one segment containing Silk/Catalase/PEG_{400} and the other segment containing Silk/PEG_{400}. (B) Janus silk swimmer made up of one segment containing Silk/Catalase/PEG_{400}, a barrier layer of PMMA (10 layers), and the other segment containing Silk/PEG_{400}.*

Conclusions

RIJ offers a versatile and easy way to be able to generate micro-motor devices such as the rockets described here, which are capable of swimming in a variety of media containing H_2O_2 fuel via a bubble propulsion mechanism. By using RIJ we are capable of generating a large variety of micro-motors by using a variety of inks, which can be digitally defined. By increasing the RSF concentration to 30 mg/ml we show the production of rigid stable micro-motors. We also show that the addition of PEG_{400} allows for a better bubble release and also diminishes the accumulation of enzyme residue on the orifice, thus enabling longer printing times without the need for frequent cleaning. Finally we show that due to the porous nature of silk the addition of 10 layer of PMMA between inactive and active parts of micro-motors helps to discourage the bubble release into the inactive half of the micro-motors and therefore allows for better trajectory control.

Experimental

Preparation of silk fibroin solution

Bombyx mori silk was degummed in order to remove sericin by briefly boiling the raw silk for 30 minutes in (0.02 M) sodium carbonate (Na_2CO_3) (99.5 % Alfa Aesar). The degummed silk was rinsed with deionized water until the solution was clear and then dried at 60 °C overnight in a drying oven.

The dried silk fibroin was dissolved in Ajisawa's reagent ($CaCl_2$ (93 % Sigma-Aldrich) / ethanol (99.8 % Sigma) / water in a 1:2:8 molar ratio) [42] at 75°C for 3 hours and was left to cool down at room temperature before being dialysed against deionized water until the solution recorded a conductivity of less than 1 µS. The dialysed silk fibroin solution was then centrifuged at 5,000 rpm for 15 mins in order to remove any particulates and fibres.

Preparation of different ink solutions

Amorphous bovine liver catalase powder (purity 60%, 5000-6000 U/mg, Sigma-Aldrich) was dissolved in deionised water at a concentration of (20 mg/ml) and then filtered with a (0.7 µm) glass filter. The following inks were the ones used for the final optimised Janus silk rockets, other inks were made by altering specific concentrations.

Ink A (for printing the rear end (active part) of the Janus micro-rockets): Catalase (CAT) solution was carefully blended (by inverting the vial several times) with PEG_{400} RSF solution to give final concentrations of (4 mg/ml CAT), (10 mg/ml) PEG_{400} and (30 mg/ml) RSF.

Ink B (for printing the barrier layers of the Janus micro-rockets): Poly methyl methacrylate (PMMA) from Sigma-Aldrich (MW/~15000) was dissolved in N, N-Dimethylformamide (Sigma-Aldrich 99.8%) (DMF) with a concentration of 10% wt/V (PMMA/DMF).

Ink C (for printing the front end (inactive part) of the Janus micro-rockets): RSF solution was carefully blended with PEG_{400} to give final concentrations of (30 mg/ml) RSF and (12 mg/ml) for PEG_{400}. The PEG_{400} concentration was chosen to be slightly higher for the part containing only silk as it discouraged bubbles sticking to the inactive side.

Ink D (for transforming RSF into β-sheet structure): (98.99%) pure methanol (Sigma).

Inkjet printing process

A MicroFab "Drop on Demand" printer with JetLab software (MicroFab Technologies, Version 6.3, build 4.0.18.3011) and four single nozzled print heads (with nozzle diameter of 60 µm) were used for the printing.

5 x 10 dot matrices were programmed into JetLab software and columns of a total height of 500 layers of silk inks (ink A

or C) were printed layer-by-layer (LBL), which equated to total heights of 250~300 μm. Ink D was printed between each silk layer to transfer the soluble silk inks into insoluble β-sheet structure.

The micro-rockets were printed on clean silicon wafers. For the fully active micro-rockets, ink A and D (500 layers of each ink) were alternatively printed. In the case of Janus micro-rockets, ink A and D (250 layers of each ink) were alternatively printed for the rear end of the Janus micro-rockets. A barrier layer of 10 layers of PMMA (ink B) was then printed on top in order to decrease the amount of bubbles leaking from the active half to the inactive half. And finally, ink C and D (250 layers of each ink) were alternatively printed to form the front end of the Janus micro-rockets. This process generated Janus particles that were half active (the rear end) and half inactive (the front end). Device optimisation experiments found that using 250 layers for inks C and D gave well defined "rocket" type aspect ratios, similar to those used in other directional swimming devices such as bi-metallic nanorods. PMMA layer thickness was also optimised with the aim to find the minimum number of layers required to prevent bubbles diffusing into the inactive side of the rockets.

Particle preparation of silk – based micromotors

Silicon wafers with printed micro-rockets were incubated in filtered (0.2 μm glass filter) deionized water, which was then carefully removed via a Pasteur pipette, ensuring the printed micro-rockets were not detached from the surface. Any dust and silk that was not in β-sheet form was removed in this washing step. This process was repeated 3 to 5 times.

After washing the Si-wafers were placed in a small beaker and the surface was covered with deionized water and held in the centre of a sonicator (2L 50W Bath sonicator – Eumax) for < 30 seconds until all or most columns were detached from the wafers. The recovered yield of micro-rockets was upwards of 80%. We qualitatively observed that detachment immediately after manufacture gave the highest yield, approaching 100%. The brief sonication process did not show any signs of damaging the rockets. The micro-rocket columns were then transferred into a petri dish (6 cm in diameter) containing 5% wt/V hydrogen peroxide and imaged under a microscope with a connected PixeLink camera, or under a PixeLink camera with a camera lens attached. Movies were taken at a frame rate of 25 frames per second (fps) for 500 to 1000 frames.

Author Biography

David Alexander Gregory has previously completed his BSc at Lancaster University in Physics with Astrophysics and Cosmology, followed by a BSc at Keele University in Biochemistry and Music. He then went on to do an MSc in Bio-nanotechnology at the University of Sheffield and Leeds University followed by a PhD project on Micro and Nano self-motile particles for which he is currently waiting on his Viva. Currently he works for Dr Xiubo Zhao as PDRA at the University of Sheffield.

References

[1] M. Leoni, J. Kotar, B. Bassetti, P. Cicuta, and M. C. Lagomarsino, "A basic swimmer at low Reynolds number," *Soft Matter,* vol. 5, pp. 472-476, 2009.

[2] A. Najafi and R. Golestanian, "Propulsion at low Reynolds number," *Journal of Physics-Condensed Matter,* vol. 17, pp. S1203-S1208, Apr 13 2005.

[3] S. Duhr and D. Braun, "Why molecules move along a temperature gradient," *Proceedings of the National Academy of Sciences of the United States of America,* vol. 103, pp. 19678-19682, Dec 2006.

[4] F. Julicher and J. Prost, "Generic theory of colloidal transport," *European Physical Journal E,* vol. 29, pp. 27-36, May 2009.

[5] S. Ebbens, D. A. Gregory, G. Dunderdale, J. R. Howse, Y. Ibrahim, T. B. Liverpool*, et al.*, "Electrokinetic effects in catalytic platinum-insulator Janus swimmers," *EPL (Europhysics Letters),* vol. 106, p. 58003, 2014.

[6] L. Baraban, D. Makarov, R. Streubel, I. Mönch, D. Grimm, S. Sanchez*, et al.*, "Catalytic Janus Motors on Microfluidic Chip: Deterministic Motion for Targeted Cargo Delivery," *ACS Nano,* vol. 6, pp. 3383-3389, Apr 24 2012.

[7] L. Soler and S. Sanchez, "Catalytic nanomotors for environmental monitoring and water remediation," *Nanoscale,* vol. 6, pp. 7175-7182, 2014.

[8] W. Gao, X. Feng, A. Pei, Y. Gu, J. Li, and J. Wang, "Seawater-driven magnesium based Janus micromotors for environmental remediation," *Nanoscale,* vol. 5, pp. 4696-4700, 2013.

[9] L. Soler, V. Magdanz, V. M. Fomin, S. Sanchez, and O. G. Schmidt, "Self-Propelled Micromotors for Cleaning Polluted Water," *Acs Nano,* vol. 7, pp. 9611-9620, Nov 2013.

[10] J. Li, V. V. Singh, S. Sattayasamitsathit, J. Orozco, K. Kaufmann, R. Dong*, et al.*, "Water-Driven Micromotors for Rapid Photocatalytic Degradation of Biological and Chemical Warfare Agents," *ACS Nano,* vol. 8, pp. 11118–11125, 2014.

[11] J. Orozco, G. Cheng, D. Vilela, S. Sattayasamitsathit, R. Vazquez-Duhalt, G. Valdes-Ramirez*, et al.*, "Micromotor-Based High-Yielding Fast Oxidative Detoxification of Chemical Threats," *Angewandte Chemie-International Edition,* vol. 52, pp. 13276-13279, Dec 9 2013.

[12] Z. Ghalanbor, S. A. Marashi, and B. Ranjbar, "Nanotechnology helps medicine: Nanoscale swimmers and their future applications," *Medical Hypotheses,* vol. 65, pp. 198-199, 2005 2005.

[13] D. A. Gregory, A. I. Campbell, and S. J. Ebbens, "Effect of Catalyst Distribution on Spherical Bubble Swimmer Trajectories," *The Journal of Physical Chemistry C,* vol. 119, pp. 15339-15348, 2015/06/10 2015.

[14] J. R. Howse, R. A. L. Jones, A. J. Ryan, T. Gough, R. Vafabakhsh, and R. Golestanian, "Self-motile colloidal particles: From directed propulsion to random walk," *Physical Review Letters,* vol. 99, Jul 27 2007.

[15] S. Ebbens, M. H. Tu, J. R. Howse, and R. Golestanian, "Size dependence of the propulsion velocity for catalytic Janus-sphere swimmers," *Physical Review E,* vol. 85, Feb 2012.

[16] S. J. Ebbens, G. A. Buxton, A. Alexeev, A. Sadeghi, and J. R. Howse, "Synthetic running and tumbling: an autonomous navigation strategy for catalytic nanoswimmers," *Soft Matter,* vol. 8, pp. 3077-3082, 2012.

[17] R. Golestanian, T. B. Liverpool, and A. Ajdari, "Propulsion of a molecular machine by asymmetric distribution of reaction products," *Physical Review Letters,* vol. 94, Jun 10 2005.
[18] J. G. Gibbs and Y. P. Zhao, "Autonomously motile catalytic nanomotors by bubble propulsion," *Applied Physics Letters,* vol. 94, Apr 20 2009.
[19] L. Li, J. Wang, T. Li, W. Song, and G. Zhang, "Hydrodynamics and propulsion mechanism of self-propelled catalytic micromotors: model and experiment," *Soft Matter,* vol. 10, pp. 7511-7518, 2014.
[20] V. M. Fomin, M. Hippler, V. Magdanz, L. Soler, S. Sanchez, and O. G. Schmidt, "Propulsion Mechanism of Catalytic Microjet Engines," *Ieee Transactions on Robotics,* vol. 30, pp. 40-48, Feb 2014.
[21] R. J. Archer, A. I. Campbell, and S. J. Ebbens, "Glancing angle metal evaporation synthesis of catalytic swimming Janus colloids with well defined angular velocity," *Soft Matter,* vol. 11, pp. 6872-6880, 2015.
[22] J. Orozco, V. Garcia-Gradilla, M. D'Agostino, W. Gao, A. Cortes, and J. Wang, "Artificial Enzyme-Powered Microfish for Water-Quality Testing," *Acs Nano,* vol. 7, pp. 818-824, Jan 2013.
[23] D. Pantarotto, W. R. Browne, and B. L. Feringa, "Autonomous propulsion of carbon nanotubes powered by a multienzyme ensemble," *Chemical Communications,* pp. 1533-1535, 2008.
[24] S. Sengupta, D. Patra, I. Ortiz-Rivera, A. Agrawal, S. Shklyaev, K. K. Dey*, et al.*, "Self-powered enzyme micropumps," *Nature chemistry,* vol. 6, pp. 415-22, 2014-May 2014.
[25] R. Kumar, M. Kiristi, F. Soto, J. Li, V. V. Singh, and J. Wang, "Self-propelled screen-printable catalytic swimmers," *RSC Advances,* vol. 5, pp. 78986-78993, 2015.
[26] W. Zhu, J. Li, Y. J. Leong, I. Rozen, X. Qu, R. Dong*, et al.*, "3D-Printed Artificial Microfish," *Advanced Materials,* vol. 27, pp. 4411-4417, 2015.
[27] Z. Y. Li, P. Beck, D. A. A. Ohlberg, D. R. Stewart, and R. S. Williams, "Surface properties of platinum thin films as a function of plasma treatment conditions," *Surface Science,* vol. 529, pp. 410-418, Apr 2003.
[28] G. Zhao, S. Sanchez, O. G. Schmidt, and M. Pumera, "Poisoning of bubble propelled catalytic micromotors: the chemical environment matters," *Nanoscale,* vol. 5, pp. 2909-2914, 2013.
[29] H. Wang, G. Zhao, and M. Pumera, "Crucial Role of Surfactants in Bubble-Propelled Microengines," *Journal of Physical Chemistry C,* vol. 118, pp. 5268-5274, Mar 13 2014.
[30] S. Ghosh, S. Chakrabarty, D. Bhowmik, G. S. Kumar, and N. Chattopadhyay, "Stepwise Unfolding of Bovine and Human Serum Albumin by an Anionic Surfactant: An Investigation Using the Proton Transfer Probe Norharmane," *Journal of Physical Chemistry B,* vol. 119, pp. 2090-2102, Feb 12 2015.
[31] P. J. Smith and A. Morrin, "Reactive inkjet printing," *Journal of Materials Chemistry,* vol. 22, pp. 10965-10970, 2012.
[32] B. B. Mandal, A. Grinberg, E. Seok Gil, B. Panilaitis, and D. L. Kaplan, "High-strength silk protein scaffolds for bone repair," *Proceedings of the National Academy of Sciences,* vol. 109, pp. 7699-7704, May 15, 2012 2012.
[33] D. N. Rockwood, R. C. Preda, T. Yucel, X. Wang, M. L. Lovett, and D. L. Kaplan, "Materials fabrication from Bombyx mori silk fibroin," *Nature Protocols,* vol. 6, pp. 1612-1631, Oct 2011.
[34] B. Kundu, R. Rajkhowa, S. C. Kundu, and X. Wang, "Silk fibroin biomaterials for tissue regenerations," *Advanced Drug Delivery Reviews,* vol. 65, pp. 457-470, Apr 2013.
[35] H. J. Jin, J. Park, V. Karageorgiou, U. J. Kim, R. Valluzzi, and D. L. Kaplan, "Water-stable silk films with reduced β-sheet content," *Advanced Functional Materials,* vol. 15, pp. 1241-1247, Aug 2005.
[36] H. J. Jin and D. L. Kaplan, "Mechanism of silk processing in insects and spiders," *Nature,* vol. 424, pp. 1057-1061, Aug 2003.
[37] C. Vepari and D. L. Kaplan, "Silk as a biomaterial," *Progress in Polymer Science,* vol. 32, pp. 991-1007, Aug-Sep 2007.
[38] A. Motta, L. Fambri, and C. Migliaresi, "Regenerated silk fibroin films: Thermal and dynamic mechanical analysis," *Macromolecular Chemistry and Physics,* vol. 203, pp. 1658-1665, Jul 2002.
[39] D. A. Gregory, Y. Zhang, P. J. Smith, S. J. Ebbens, and X. Zhao, "Reactive Inkjet Printing of Biocompatible Enzyme Powered Silk Micro-Rockets," *Small, DOI: 10.1002/smll.201600921,* 2016.
[40] K. A. Burke, D. C. Roberts, and D. L. Kaplan, "Silk Fibroin Aqueous-Based Adhesives Inspired by Mussel Adhesive Proteins," *Biomacromolecules,* vol. 17, pp. 237-245, Jan 2016.
[41] D. J. Wesley, R. M. Smith, W. B. Zimmerman, and J. R. Howse, "Influence of Surface Wettability on Microbubble Formation," *Langmuir,* vol. 32, pp. 1269-1278, Feb 2016.
[42] A. Ajisawa, "Dissolution of silk fibroin with calciumchloride/ethanol aqueous solution," *The Journal of Sericultural Science of Japan,* vol. 67, pp. 91-94, 1998.